Journal of Applied Polymer Science

Preparation of nonwoven mats of electrospun poly(lactic acid)/polyaniline blend nanofibers: A new approach

Mazen Al-Jallad, Yomen Atassi
Department of Physics, Higher Institute for Applied Science and Technology, P.O. Box 31983, Damascus, Syria
Correspondence to: Y. Atassi (E-mail: yomen.atassi@hiast.edu.sy)

ABSTRACT: The preparation of nonwoven mats of electrospun poly(lactic acid)/polyaniline (PANI) blend nanofibers faces some critical challenges that will be addressed in the present work. The challenges are in achieving high and adjustable content of PANI while keeping the spinnable solution nonagglomerated with no need to further filtration that might lead to wrong estimation of PANI content in the mat. We report an unprecedented content of 40% wt of PANI that is achieved using a new two-step procedure. It is based on: (1) the preparation of the spinnable solution from a friable nonagglomerated and readily dispersible PANI:*p*-TSA powder and (2) the use of an optimized mixture of *m*-cresol/dichloromethane. The obtained nanofiber mats are characterized by FTIR and UV–vis spectroscopy. The morphology and the thermal stability of the nanofibers are investigated by scanning electron microscopy (SEM) and differential scanning calorimetry (DSC). The amorphous structure of the nanofibers is verified using XRD measurements. The DC-conductivity of these blend nanofibers is found to be far larger than the published DC-conductivity values for blend nanofibers of PANI with PLLA or with other polymers. This is attributed to the high content of PANI in the blend and to the role played by *m*-cresol as a secondary dopant. The investigation of the aging effect on the DC-conductivity reveals an exponential decrease with a characteristic time of $\tau \approx 13$ weeks. The electrical impedance spectroscopy (EIS) shows a pure ohmic behavior of the blend mat. © 2016 Wiley Periodicals, Inc. J. Appl. Polym. Sci. **2016**, *133*, 43687.

KEYWORDS: biomaterials; blends; conducting polymers; electrospinning

Received 23 June 2015; accepted 23 March 2016
DOI: 10.1002/app.43687

INTRODUCTION

Inherently conductive polymers have recently gained great attention as promising candidates for applications such as solar cells,[1,2] energy harvesting,[3,4] sensing devices,[5,6] actuators,[7,8] light emitting diodes,[9] and electromagnetic interference shielding.[10,11]

Polyaniline (PANI) is one of the most investigated inherently conductive polymers, because of its unique properties and characteristics, namely, its ease of preparation, simple reversible doping/redoping, good environmental stability, and relatively low-cost monomer. Most of the potential applications of PANI use its nanostructure, especially nanofibers.[12,13] However, a major limitation to its commercial applications comes from its poor solubility and processability as it has a fairly rigid backbone because of its high aromaticity. The elasticity of its solutions is generally insufficient to be electrospun directly into fibers.[14,15] Therefore, different approaches have been proposed to prepare PANI nanofibers, such as interfacial polymerization,[16,17] seeding polymerization,[4,5] coating polyaniline onto a nonconducting nanofiber substrates using bulk oxidative solution polymerization process,[18,19] and electospinning PANI blends with more flexible, high molecular weight polymers that act as processing aids.[2,14]

Within the electrospinning process, the poor solubility of PANI makes its blend solutions considered dispersions rather than true ones.[15] This leads to an unstable and discontinuous electrospinning process, where the resulting fibers have nonhomogeneous physical and electrical properties. Many solutions were investigated to enhance the solubility of PANI in blend solutions, namely, copolymerizing aniline with substituted anilines,[20,21] using polar solvents or a mixture of polar solvents such as tetrahydrofurn, hexafluropropan-2-ol and chloroform[14,22] or using protonic organic acids dopants such as camphor sulfonic acid (CSA),[14,23] para-toluene sulfonic acid (*p*-TSA),[24,25] or dodecylbenzen sulfonic acid (DBSA).[26] In spite of all these attempts, the solubility of PANI is still low.[27,28]

Moreover, the spinnable solution needs further filtration prior to the electrospinning process to remove non soluble residues. Otherwise, they might cause distortion of Taylor cone,

Additional Supporting Information may be found in the online version of this article.

instability of the spinning jet, or nozzle clogging which stops the spinning process.[2] However, the filtration of the spinnable solution makes the estimation of the content of PANI in the final blend mat difficult and makes the fine tuning of the electrical conductivity of the resulting mat infeasible.[23,29–31] Generally, the conductivity of PANI blend nanofiber mat increases 10 folds for every one fold increment in PANI weight content in the mat.[14,32,33] For applications such as tissue engineering, actuators and chemical sensors, blend mats that possess a high and tunable electrical conductivity with a long-term stability are of great importance.

The goal of this work is to present a new procedure for the preparation of electrospun nanofibers in the form of nonwoven mat from *p*-toluene sulfonic acid-doped polyaniline, PANI:*p*-TSA, blended with poly(lactic acid) that overcome the aforementioned problems; i.e., the content of PANI:*p*-TSA in the spinnable solution is high and tunable. Furthermore, the spinnable solution needs no filtration prior to the electrospinning process.

This new procedure consists of a two-step approach (1) the preparation of a friable and readily dispersible PANI:*p*-TSA powder and (2) the use of an optimized mixture of *m*-cresol/dichloromethane (DCM) solvents.

The present study also aims at achieving a good intercalation, of as high as 40% wt, of PANI in PLLA matrix. This would significantly increase the conductivity of the blend nanofiber mat with superior mechanical properties endowed by the host matrix. The resulted mat has potential applications in chemical sensors and can be used as scaffold in tissue engineering.

EXPERIMENTAL

Reagents and Chemicals

Polylactic acid (PLLA, $M_w = 150{,}000$ g/mol) from NatureWorks (Minnetonka, USA) was kindly offered by ENSAM/PIMM laboratory (Paris, France). Anilinium chloride monomer, *p*-toluene sulfonic acid, tetra n-butyl ammonium bromide (TBAB), ammonium peroxydisulfate [$(NH_4)_2S_2O_8$, APS], chloroform, dichloromethane, and ethanol were purchased from Merck (Darmstadt, Germany). *m*-cresol was purchased from Fluka (Buchs, Switzerland). All chemicals were of analytical reagent grade and were used as received without further purification.

Synthesis of Friable, Nonagglomerated, Dispersed Powder of PANI:*p*-TSA

Typically (5.18 g, 40 mmol) of aniline hydrochloride is dissolved in 100 mL of deionized water with the aid of ultrasonication. Ammonium peroxydisulfate (APS) (11.42 g, 50 mmol) is dissolved in 100 mL of deionized water using magnetic stirring. Both solutions are kept for 1 h at room temperature (~20–24 °C). The APS solution is then added drop-wise to the above mixture under ultrasonic stirring for 30 min. The mixture is left for 24 h under magnetic stirring to insure that most of aniline monomers had been consumed and the polymerization reaction is almost finished. The resulting PANI:Cl (ES) is then filtered and washed repeatedly with deionized water keeping the PANI paste wet (to prevent aggregation of PANI:Cl when it gets in contact with air). The washing is repeated until the water washings are colorless with pH 7. The wet PANI paste is then transferred to a 100 mL solution of 1M NH_4OH with magnetic stirring for 24 h to obtain the emeraldine base (EB) form of PANI. The (EB) solution of PANI is filtered and washed with deionized water until the water washings are colorless with pH 7. We have to point out that the PANI (EB) paste is always kept wet. The losses of mass in PANI:Cl and PANI-base, when filtering on filtration paper, were taken into account by weighing precisely the filter paper before using and after drying it in each filtration step. These measurements allow to accurately calculate the amount of *p*-TSA needed to prepare PANI:*p*-TSA (ES).

Finally, the wet (EB) paste is transferred into 100 mL of ethanol in a closed vessel. The solution becomes instantly dark violet and homogeneous. *p*-TSA is then added to the solution in a stoichiometric amount to obtain PANI:*p*-TSA (ES). The solution is left for 24 h under magnetic stirring. It becomes dark green. After that, the vessel is opened and put in a desiccator at 40 °C for 24 h for drying. A green, friable, nonagglomerated powder is then collected and preserved in a closed vessel in the dark.

Preparation of PLLA/PANI Blend Nanofiber Nonwoven Mats

0.2 g of PANI:*p*-TSA powder is dissolved in 1 mL of *m*-cresol and 4 mL of DCM mixture with ultrasonication aid for 15 min, then 0.3 g of PLLA granules is added to the above solution and left under magnetic stirring for 6 h. The electrical conductivity of spinnable PLLA/PANI solution is 800 μS cm^{-1} measured by conductivity meter (JENWAY-4510-Staffordshire, UK) at 24 °C. Polymers blend solution is added to 10 mL glass syringe with hypodermic needle used as nozzle. The inner and outer diameter of the needle is 0.6 and 0.8 mm, respectively. The flow of the spinnable solution was controlled using a programmable syringe pump (TOP-5300, Tokyo, Japan). The high-voltage power supply is an ES813-D50.1 Dual output: 0 to ±50 kV/1 mA Electrostatic/HV Generator (Rolla, MO, USA). The collector is a sheet of aluminum (40 × 25 × 0.4 cm) covered with an aluminum foil.

The solution feed rate is kept at 0.4 mL h^{-1} and the distance between the collector and the needle tip is maintained at 20 cm.

The stable jets are launched as the high voltage reached 20 kV, and the surface tension of the polymer solution is overcome by the electric force acting on the Taylor cone producing green nanofibers adhering smoothly to the collector. The voltage is held at 20 kV during the experiment. The temperature inside the electrospinning chamber is kept at 22 ± 2 °C, and the relative humidity is maintained between 40 and 50% to have good evaporation of the solvents. The duration of each electrospinnig process is about five hours.

The as-spun fibers on the aluminum foil are then dried in a desiccator at 40 °C for 24 h to dispose of the residual traces of *m*-cresol. The green nonwoven mat is then peeled carefully and stored in a closed vessel in the dark for further characterizations.

Preparation of PLLA Nanofiber Nonwoven Mats

PLLA nanofibers are prepared according to the procedure mentioned in our previous work[19] and is also described in the

Supporting Information. The aim of this preparation is to compare the physical characteristics of PLLA nanofibers with those of PLLA/PANI blend nanofibers.

Characterization

PLLA and PLLA/PANI Blend Nanofiber Mats Morphology. The nanofibers morphology is analyzed using Tescan Vega-II XMU5136 variable pressure scanning electron microscopy (SEM) (El-Segundo, CA, USA). Samples are coated with graphite to increase the clarity of the SEM micrographs using EMITECH K975 carbon evaporator (Quorum, Laughton, UK).

Nanofiber mat thickness is measured using a digital micrometer (Mitutoyo CLM1 Yokohama, Japan) and the nanofibers diameters are measured using Image-J software.

X-ray Diffraction (XRD) Measurements. XRD patterns are performed with PHILIPS-PW3710 X-ray diffractometer (Amsterdam, Netherlands) operating at 60 kV using Cu-K_α radiation ($\lambda = 0.154$ nm). X-ray diffractograms are recorded in the 2θ range: 5–60°.

Differential Scanning Calorimetry (DSC). DSC analysis is carried out with a computerized SETARAM-INSTRUMENTATION TGA-DSC (Caluire, France). Samples are heated to 200 °C at a ramping rate of 10 °C/min in nitrogen atmosphere. Crystallinity of PLLA in PLLA nanofiber mats and in PLLA/PANI blend nanofiber mats is calculated according to the following equation[34]:

$$\text{Crystallinity } (\%) = \frac{\Delta H_m - \Delta H_{cc}}{\Delta H_m^0 \times C}, \quad (1)$$

where ΔH_m and ΔH_m^0 are the endothermic enthalpy of the samples and that of 100% crystallized PLLA ($\Delta H_m^0 = 93$J/mol), respectively.[34] ΔH_{cc} is the enthalpy of cold crystallization and C is the PLLA mass percentage (m%) in the tested sample.

FTIR Spectroscopy. FTIR spectra are recorded by BRUKER-VECTOR22 FTIR spectrophotometer (Billerica, MA, USA). Samples of PLLA nanofiber mats and PLLA/PANI blend nanofiber mats are fixed on the support directly on the path of the optical beam. PANI:*p*-TAS powder is mixed with KBr and compressed in pellets. All spectra are corrected for the presence of moisture and carbon dioxide in the optical pathway.

UV–vis Spectroscopy. UV–vis spectra are recorded by JASCO V-350 UV–vis spectrophotometer (Tokyo, Japan) in a wavelength range of 300–1100 nm. Samples of PLLA nanofiber mats and PLLA/PANI blend nanofiber mats are held perpendicularly to the path of the beam. PANI:*p*-TSA powder is dissolved in 1:4 v/v (*m*-cresol/DCM) mixture in a quartz cell.

Electrical Measurements. DC-conductivity (σ) measurement is performed using a four-probe technique, where PLLA/PANI blend nanofiber mats is tested using a four-probe homemade device consisting of four parallel contacts positioned 2 mm away from each other. Each contact is made of five adjacent platinum wires of 0.1 mm diameter. The contact length of each probe is 3 cm. KEITHELY-220 (Bracknell, UK) is used as a programmable current source and KEITHELY-617 is used as a programmable electrometer. Twenty kilopascal pressure is applied on the upper surface of the mat to achieve a good contact between the mat and the electrodes.

σ is calculated using Van der Pauw's relation $\sigma = \frac{d}{t \times w} \frac{I}{V}$, where d is the distance between the electrodes (cm) and t and w are the sample thickness and width, respectively (cm).

The conductivity of PANI:*p*-TSA powder is measured by the conventional four-point Van der Pauw method on pellets of 13 mm in diameter compressed at 700 MPa with a manual hydraulic press, using the relation $\sigma = \frac{1}{2\pi s} \frac{I}{V}$, where s is the distance between two adjacent point-probe (cm) ($s = 0.156$ cm in our set-up).

DC-conductivity is measured over the period of 30 weeks (one measurement per week) to evaluate the conductivity degradation of the blend nanofiber mats.

Electrical impedance spectroscopy (EIS) spectra are investigated by computerized Hewlett-Packard 192A-LF impedance analyzer (Miami, FL, USA) in the range 5 Hz–13 MHz to reveal Nyquist and Bode blots of the mats, using a capacitive impedance cell. Samples were cut in circular form of 25 mm diameter and entered into the teflon cavity. The distance between the two circular aluminum electrodes is controlled to be the same as the sample thickness measured by the digital micrometer (Mitutoyo CLM1) to prevent over-pressure on the sample. The input signal is sinusoidal with 1 V amplitude. Photos of the four-probe device and the capacitive impedance cell are presented in the Supporting Information.

RESULTS AND DISCUSSION

Synthesis of Friable, Nonagglomerated, Dispersed Powder of PANI:*p*-TSA

Usually, PANI-base powder is the starting material when preparing most of PANI blend spinnable solutions since the chloride ion is considered to be a bad counter-ion when dissolving PANI,[14,23,24,31] due to the hardly agglomerated PANI:Cl powder [Figure 1(a)]. PANI-base is mostly redoped with CSA or *p*-TSA or DBSA. But, it is also a gritty, agglomerated and nonreadily dispersed powder[35] [Figure 1(b)]. It needs very fine grinding and long agitation time to achieve a reasonable solubility, followed by further filtration before electrospinning. This leads to a difficult estimation of polyaniline percentage in the final blend as we mentioned in the introduction.[23,29–31]

We found experimentally that ethanol is a good dispersing agent for PANI-base paste (i.e., wet PANI-base before being clustered). Indeed, it is a protic solvent with good affinity to PANI. With this agent PANI chains become more spaced because of possible hydrogen bonds between ethanol and PANI. Moreover, it allows *p*-TSA molecules to be easily dispersed inside PANI cluster and to form polar bonds with nitrogen atoms of PANI. On the other hand, as *p*-TSA molecule has a long alkyl chain, it keeps sufficient distance between PANI chains that prevents hard agglomeration of the resulting powder when ethanol evaporates. Therefore, the prepared PANI:*p*-TSA powder is nonagglomerated, friable, and readily dispersible [Figure 1(c)].

Optimization of PLLA/PANI:*p*-TSA Spinnable Blend Solution and Electrospinning Parameters

Problems such as the distortion of Taylor cone, instability of the spinning jet and nozzle clogging which stops the spinning

Figure 1. Photos of nonfriable and hard agglomerated powder of (a) PANI:Cl, (b) PANI-base. (c) As-dried friable and nonagglomerated PANI:*p*-TSA powder. [Color figure can be viewed in the online issue, which is available at wileyonlinelibrary.com.]

process, hinder the electrospinning of PLLA/PANI blend solution with high content of PANI. These problems arise from the poor solubility of PANI which leaves insoluble residues that render the spinnable solution nonhomogeneous. Two steps are proposed to overcome these problems:

First, the preparation of a readily dispersible powder of PANI:*p*-TSA as described before. Second, the selection of an appropriate solvent. *m*-cresol is chosen because it is one of the most effective solvents of PANI.[36,37] In fact, the small size of *m*-cresol facilitates its diffusion into PANI cluster. Moreover, as it has the ability to exchange a proton with a *p*-TSA ion and PANI, it plays the role of a secondary dopant that modifies the conformation of PANI from a more coil-like to a more expanded conformation.[37] Further, the possible formation of hydrogen bonds between the dopant and the solvent results in larger interchain distance. This leads to a higher solubility of PANI.[36] But, as *m*-cresol has a high boiling temperature (202.8 °C) and low vapor pressure (~1 mm Hg at 20 °C), it is impossible to realize fiber formation from PLLA/PANI blend solution using this solvent alone.

To address this issue, we firstly chose the widely used chloroform as a second solvent[14,31,38,39] (boiling point: 60.5–61.5 °C, vapor pressure: 160 mm Hg at 20 °C, dipole moment: 1.04 D, and dielectric constant: 4.8).

The use of chloroform did not give good results. Indeed, a high solubility of 40% wt of PANI in the 10% w/v PLLA/PANI blend solution was achieved just when 1.5:4 v/v of (*m*-cresol/chloroform) solvent mixture was used. But with this formulation, the solution was only electro-sprayed and no fiber was formed [Figure 2(a)]. The fiber formation began at 1:4 v/v (*m*-cresol/chloroform) solvent mixture. Here again, the blend solution was not homogeneous [Figure 2(b)] and some PANI particles were present in the resulting mat [Figure 2(c)]. The insoluble particles in the blend solution resulted in unstable jet and over loaded of the syringe pump because of the nozzle clogging. This stopped the electrospinning process a short time after.

To deal with this problem, we chose dichloromethane (DCM). It has a low boiling point temperature (39.8 °C), a high vapor pressure (353 mm Hg at 20 °C), a suitable dipole moment of 1.6 D, and a dielectric constant of 9.1.

The use of DCM enables easier tuning of volume ratio of *m*-cresol in the solvent mixture rather than chloroform, knowing that DCM is also considered as the best solvent for PLLA.

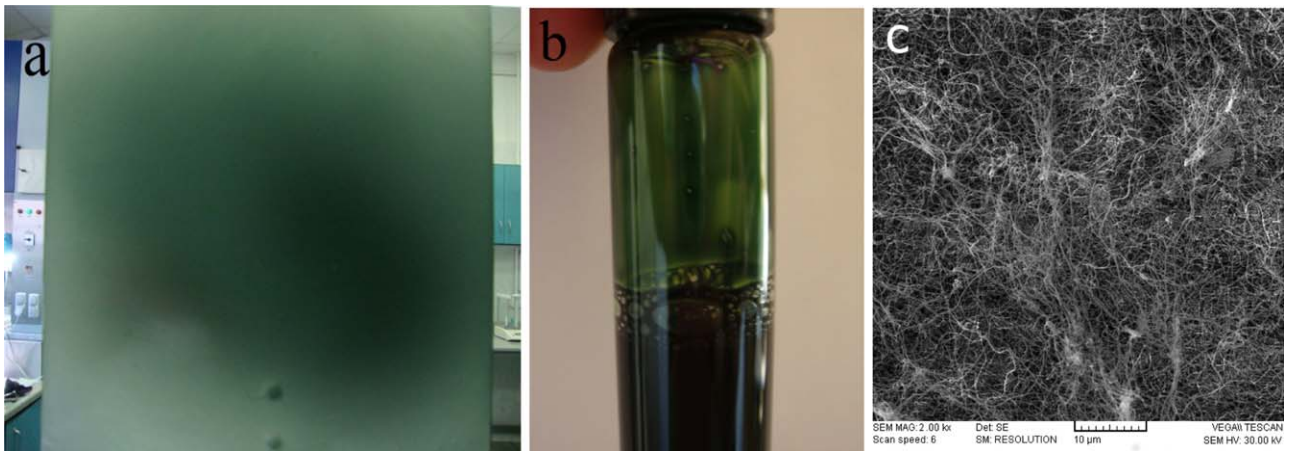

Figure 2. (a) Electro-sprayed film on the substrate of 3:2 w/w (PLLA/PANI:*p*-TSA) in 1.5:4 v/v (*m*-cresol/chloroform) solvent mixture. (b) 3:2 w/w (PLLA/PANI:*p*-TSA) in 1:4 v/v (*m*-cresol/chlorform) solvent mixture and (c) micrograph of the resulting mat from the blend solution of (b). [Color figure can be viewed in the online issue, which is available at wileyonlinelibrary.com.]

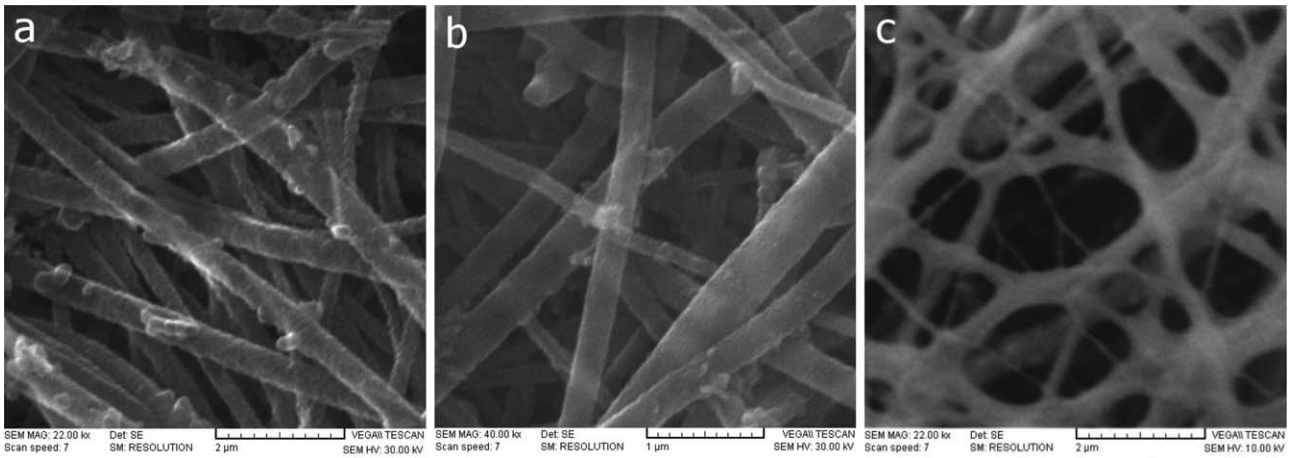

Figure 3. SEM micrographs of PLLA/PANI blend nanofibers in (*m*-cresol/DCM) solvent mixture: (a) 0.5:4 v/v, (b) 0.75:4 v/v and (c) 1.25:4 v/v concentrations.

The preliminary experiments on this solvent revealed that the best mats were produced when 1:4 v/v (*m*-cresol/DCM) solvent mixture was used for 10% w/v blend solution of 3:2 w/w (PLLA/PANI). The use of lower ratio of *m*-cresol than that mentioned above leads to uncompleted solubility of PANI, where insoluble particles of PANI were presented in the mat [Figure 3(a,b)], accompanied with technical difficulties in the electrospinning process such as the instability of the polymer solution jet and overloaded of the syringe pump and frequent nozzle clogging. Also, the use of higher ratio of *m*-cresol in the solution mixture resulted in welded nanofibers [Figure 3(c)] because of the presence of un-evaporated traces of *m*-cresol in the fibers, the nonwoven mats were strongly adhered to the substrate and they were hard to peel. More details concerning these preliminary experiments are discussed in the Supporting Information.

Morphology of PLLA Mats and PLLA/PANI Blend Nanofiber Mats

Nanofiber mats of PLLA have a smooth and homogeneous surface as shown in Figure 4(a). They have a circular shape of about 15 cm in diameter and about 100 μm in thickness with good mechanical toughness and a high flexibility.

SEM micrographs [Figure 4(b)] show that PLLA nanofibers are continuous, almost straight at the micrometer scale, randomly oriented, smooth and hollow, as they look very transparent with very thin nanofibers walls.[19] PLLA fibers have an average diameters of 186 ± 85 nm and they are beads free.

Blend nanofiber mats have also a smooth and homogeneous surface with a beautiful dark green color of conductive PANI emeraldine salt, as shown in Figure 4(c). The blend mats have also a circular shape of about 18 cm in diameter and about 90 μm in thickness. They exhibit good mechanical toughness and flexibility when handled during the characterization experiments.

SEM micrographs [Figure 4(d)] reveal that PLLA/PANI blend nanofibers are randomly oriented and beads free. The average diameter of PLLA/PANI blend nanofibers is 204 ± 83 nm.

DSC Characterization

DSC was employed to study the thermal properties of PLLA/PANI blend nanofibers and to find out if there is any phase segregation in these nanofibers [Figure 5(a)], knowing that the PANI:*p*-TSA content in the blend nanofibers is 40% wt.

The DSC curve of PLLA nanofiber mat reveals that the glass transition (T_g) temperature is at 53.5 °C followed by a distinctive endothermic aging peak at about 62.2 °C. A cold crystallization exothermic peak (T_{cc}) is observed at 77.7 °C and a sharp melting peak (T_m) at 167 °C.[12,30,40,41] Integrating the two peaks (T_{cc}) and (T_m) of PLLA nanofiber mat shows that they have the same absolute values ($\Delta H_m \approx \Delta H_{cc} = 44$ J/mol) which means that the melting phenomenon after the cold crystallization concerned only the PLLA crystal phase developed during the heating scan. This indicates that the electrospun PLLA nanofibers are completely amorphous as previously reported.[19,40,42]

As for PLLA/PANI blend nanofiber mat DSC curve, it shows a slight shift in temperature values mentioned above, where T_g is found at 59.6 °C followed by an aging peak at 65.3 °C. T_{cc} is shifted to 78 °C and T_m is increased to 168.4 °C. The aging peak of PANI is not observed in this spectrum since it is out of the heating range (250–260 °C).[12]

The increase in T_g (~6 °C) can be attributed to the decrease of surface/volume ratio of the blend mat compared with PLLA mat because the blend fibers diameter is bigger.[43] T_g is also related to the inner-stress resulting from the orientation of the polymer chains caused by the electrospining process.[44] In the blend mats, the presence of PANI obstructs and limits the free orientation of PLLA chains so the inner-stress decreases. Thus, as temperature rises, the movement of polymer chains driven by the inner-stress is expected to occur at a higher T_g.[30] In general, the value of T_g increases as the weight percentage of PANI in the blend nanofibers increases.[30] But this increase is sublinear, as the present PANI molecules in the blend nanofibers play the role of a thermal stabilizer like other thermal stabilizers used with PLLA.[45,46]

The increase in T_m value indicates that the presence of PANI in PLLA matrix affects the mobility of PLLA chains, because of the mutual interactions between the two polymer chains, where intermolecular hydrogen bonds can be expected.[30,47]

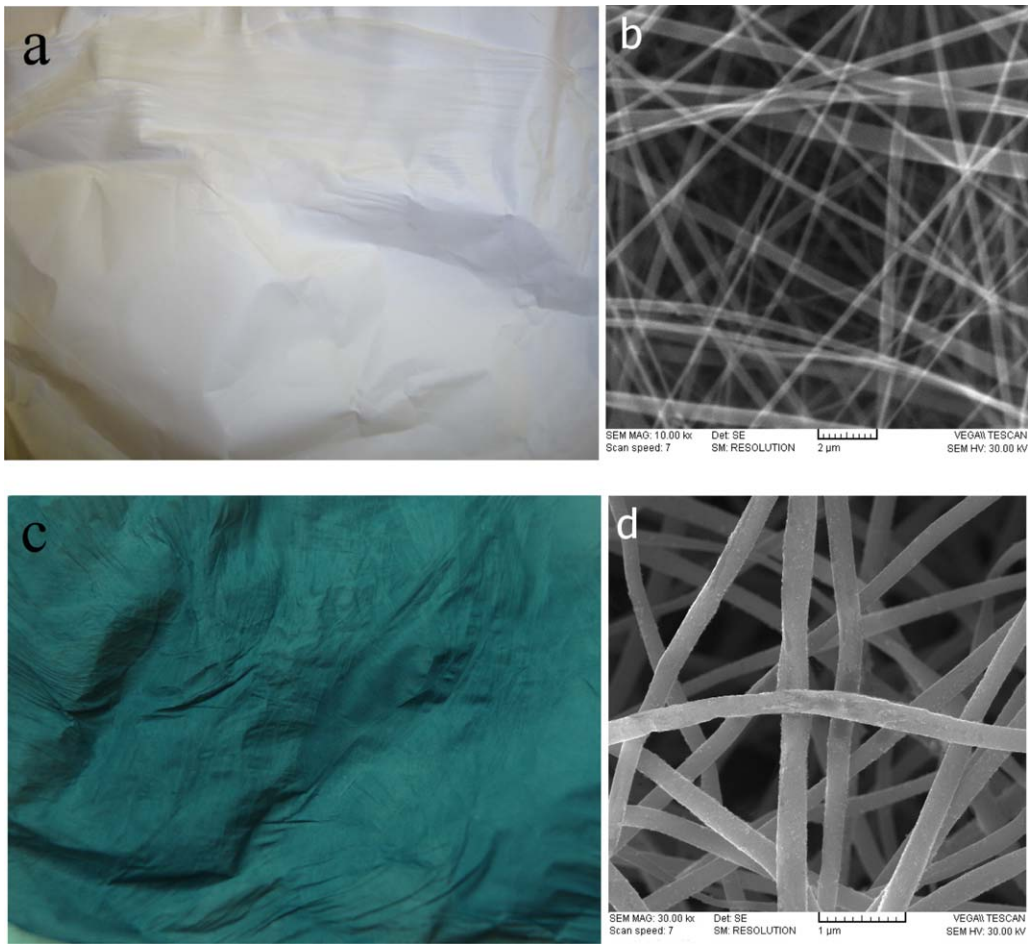

Figure 4. Photos and SEM micrographs of (a,b) PLLA nanofiber nonwoven mat and (c,d) PLLA/PANI:*p*-TSA blend nanofiber nonwoven mat. [Color figure can be viewed in the online issue, which is available at wileyonlinelibrary.com.]

Integrating the two peaks (T_{cc}) and (T_m) of PLLA/PANI nanofiber mat has proved that they also have the same absolute values ($\Delta H_m \approx \Delta H_{cc} = 32$ J/mol). As explained above, we can consider that the electrospun PLLA/PANI blend nanofibers is amorphous. This amorphous nature emphasizes the hypothesis that there is no phase segregation in these blend nanofibers, because during the electrospinning process, the polymeric jet takes only a few milliseconds to come out from the nozzle and solidify as fibers on the substrate.[2] This very fast fiber formation process restrains polymer chain mobility. Consequently, the crystalline growth is inhibited preventing any phase separation.[2]

FTIR Spectra

The FTIR spectra [Figure 5(b)] were recorded to reveal the molecular interaction between PLLA and PANI in the blend nanofibers. The main characteristic peaks of PLLA nanofiber mat and PANI:*p*-TSA powder are assigned in details in the Supporting Information.

The FTIR spectrum of PLLA/PANI blend mat exhibits the characteristic peaks of PLLA in the blend nanofibers with some shift of those of PLLA nanofibers. The two peaks of the terminal –OH groups stretching vibration are shifted down to 3710 and 3491 cm^{-1}. The peaks of C–H stretching vibration and $-CH(CH_3)$ bending vibration are situated at 2994, 2942, and 1451 cm^{-1}. The peak of $-CH_2$ stretching vibration is located at 2871 cm^{-1}. The position of the sharp peak of C=O stretching vibration did not change and it appeared at 1758 cm^{-1}. The C–O stretching vibration peak appeared at 1186 and 1091 cm^{-1} and the C–H stretching peak rested at the same position at 868 cm^{-1}.

On the other hand, all of the characteristic peaks of PANI:*p*-TSA appear in the blend nanofibers spectrum but with red shift. These peaks are situated and assigned as follows: the two peaks at 1574 and 1493 cm^{-1} are assigned to C=C stretching of quinonoid and benzenoid rings, respectively. The peaks at 1300 and 1261 cm^{-1} correspond to C–N and C–N^+ stretching vibration, respectively. The $N^+=C$ vibration is represented by the shoulder at 1124 cm^{-1}. The aromatic C–H out-of-plane bending vibration is located at 812 cm^{-1}. The shoulder at 1043 cm^{-1} is attributed to the asymmetric and symmetric O=S=O stretching vibrations of sulphonic groups. The peak at 681 cm^{-1} represents the C–S stretching. The weak band of the free N–H of the secondary amines stretching vibration is shifted up to 3230 cm^{-1}. These results are in accordance with previous literature concerning PLLA/PANI blends.[2,23,29]

The red shift in peaks positions reveals the mutual interaction between PLLA and PANI chains in the blend nanofiber and

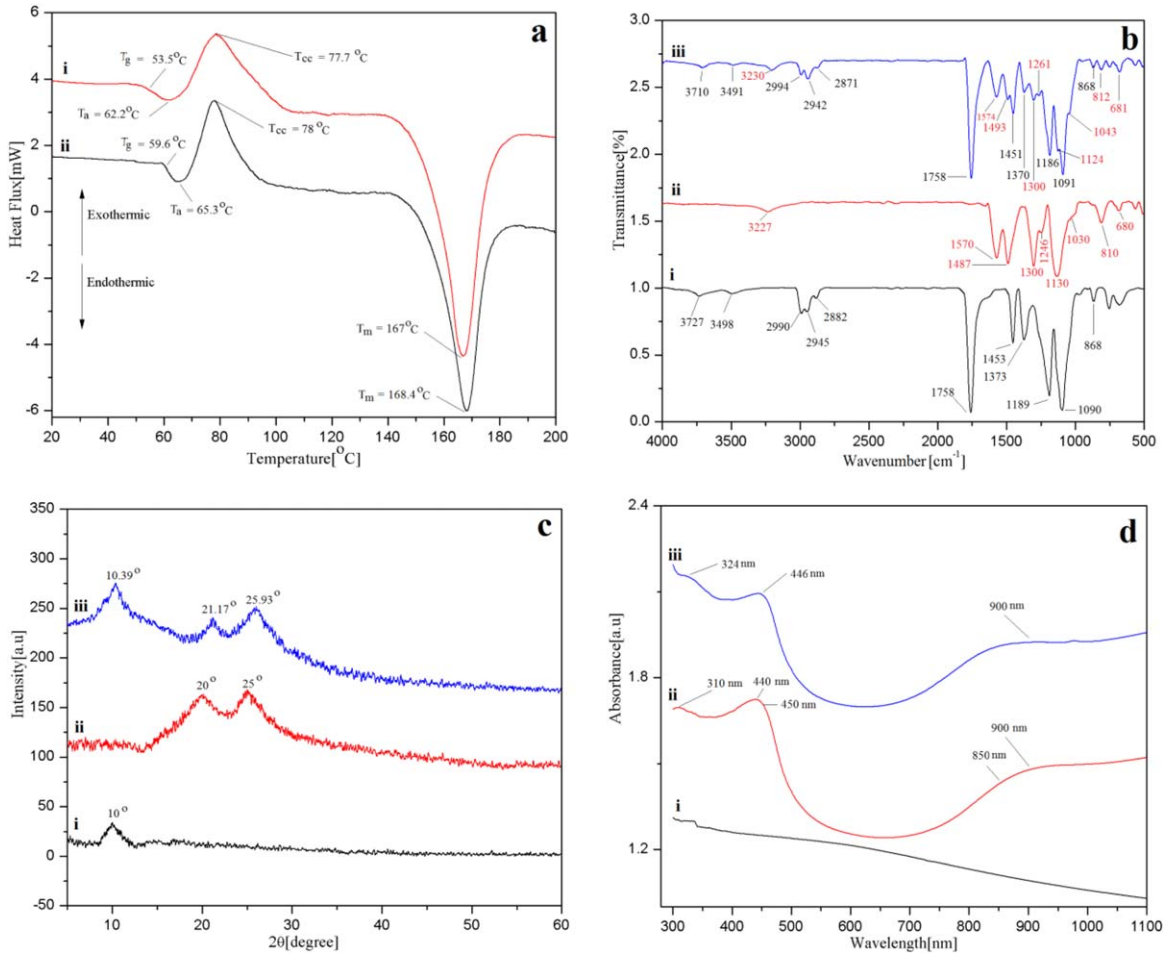

Figure 5. (a) DSC analysis of (i) PLLA nanofiber mat and (ii) PLLA/PANI blend nanofiber mat. (b) FTIR spectra, (c) X-ray diffractograms and (d) UV–vis spectra of (i) PLLA nanofiber mat, (ii) PANI:*p*-TSA powder, and (iii) PLLA/PANI blend nanofiber mat. [Color figure can be viewed in the online issue, which is available at wileyonlinelibrary.com.]

reflects the existence of intermolecular bonds between the PLLA and PANI chains. These results consolidate our assumption that PLLA/PANI nanofibers represent a compatible blend. In addition, the ratios of the intensities of PANI peaks to PLLA peaks reflect the high content of PANI in the blend nanofibers.

XRD Measurements

Figure 5(c) depicts the result of XRD measurements. The main characteristic peaks of PLLA nanofiber mat and PANI:*p*-TSA powder are discussed in details in the Supporting Information.

As for the X-ray diffractogram of PLLA/PANI blend nanofibers, it reveals the two broad peaks of PANI with about one degree shift and with less intensities. The extended halo of PLLA was slightly shifted to 10.39°. This means that the blend nanofibers also have amorphous structure. One can deduce that despite the modification of the conformation of PANI chains in the electrospun solution caused by *m*-cresol, the fast evaporation of the solvents during fiber formation induces a slight perturbation in the arrangement of PANI chains. This leaves the chains in their extended conformation (proved also by UV–vis spectroscopy and by the enhancement of the electrical conductivity of the mat) but not arranged in an aligned structure. In addition, the presence of intercalated PLLA chains with their dominant tendency to form amorphous morphology, forces the blend nanofibers to be amorphous.

UV–vis Spectroscopy. The UV–vis spectra are depicted in Figure 5(d). PLLA spectrum shows no characteristic bands with a slight decrease in the absorption intensity towards long wavelength. PLLA fibers can be considered almost transparent in the wavelength region of 300–1100 nm.[48,49]

As for PANI:*p*-TSA powder, an absorption peak at 310 nm usually assigned to the π–π^* transition of the benzeoid ring and a broad absorption valley in the range 450–850 nm are observed. The peak at 440 nm represents the polaron band-π^* transition.[13,39,50] The spectrum also shows a steadily upward trend "free carrier tail" from 900 nm to the IR region, which is characteristics of metallic conductive materials. It represents the intra-band transitions within the half-filled polaron band.[51] Actually, PANI chains have an extended conformation in *m*-cresol, so the twist defects between aromatic rings are removed. Therefore, the interaction between the adjacent polarons becomes stronger, and the polaron band becomes more dispersed in energy (i.e., more delocalized).[1]

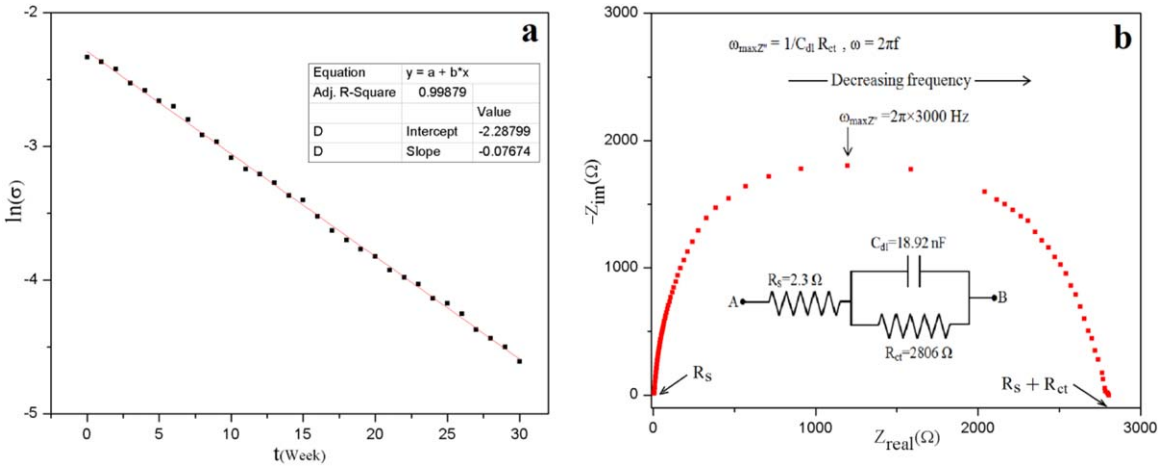

Figure 6. (a) ln(σ) as a function of time t (week) and (b) Nyquist plot with the equivalent circuit of PLLA/PANI blend nanofiber mat. [Color figure can be viewed in the online issue, which is available at wileyonlinelibrary.com.]

The UV–vis spectrum of PLLA/PANI blend nanofiber mat is similar to the spectrum of PANI powder but with some shift in peaks positions, where the peak at 310 nm is shifted to 324 nm, and the peak at 440 nm is shifted to 446 nm. The steady increasing free carrier tail at ~900 nm is still present. The similarities between the two spectra affirm that the deformation in the conformation of PANI chains from a more coil-like to a more expanded conformation due to *m*-cresol in the spinnable solution is conserved after the nanofiber formation and evaporation of solvents. This explains the enhancement in electrical properties of the blend mat as it will be discussed in the next section. Moreover, the steady increasing free carrier tail from 900 nm to IR region in the spectrum and the dark green color of PLLA/PANI blend nanofiber mat [Figure 4(c)], indicate that PANI is in its emeraldine conducting state.[1,13]

Electrical Measurements

DC-Conductivity. The DC conductivity (σ) is evaluated on virgin and newly prepared samples (powders and mats), directly after desiccation to discard the effect of aging and humidity on σ values.

The conductivity of PANI:*p*-TSA powder was 1.24 S cm^{-1}, which is about thirty times higher than other σ values reported for such powder prepared in conventional methods where $\sigma = 0.03$–0.05 S cm^{-1}.[52,53] We can attribute this improvement in σ value to the positive role played by ethanol as a dispersing agent during the redoping of PANI with *p*-TSA. In fact, it provides enough spacing between PANI chains that allows the counter ions generated form *p*-TSA to better intercalate into the polymer chains and enhance the doping efficiency of the relaxed and extended backbones of PANI(EB).

The DC-conductivity (σ) of the blend mats was found to range from 0.074 to 0.098 S cm^{-1}, where 30 measurements were carried out for each of the PLLA/PANI blend nanofiber nonwoven mats ($n = 7$ mats) prepared as mentioned above with 15 measurements on each side. We can attribute the small shift in σ between different mats to some process deviations committed during the preparation of each one, either in spinnable solutions preparation or during the electrospinning process.

Comparing σ values obtained in this work with the highest conductivity values of other blend nanofiber mats of PLLA/PANI that were prepared (by different methods), with the maximum feasible weight percent of PANI in the blend,[20,22] our σ values are two to ten times larger.

Other blend nanofiber mats of polycaprolactone (PCL) and PANI, which are also used in vivo and tissue engineering as biomaterial scaffolds,[1–3] or in chemical gas sensors,[54] had faced the same electrospinning difficulties resulting from the low solubility of PANI. The PANI weight percentage in the blend mats was limited to 30%, with conductivities in the range 7.0×10^{-4} to 0.064 S cm^{-1}, which are less than ours.

Other blend nanofiber mats of PANI with different supporting thermoplastic polymers like PEO or PMMA, had conductivities in the range 0.001–0.06 S cm^{-1},[14,55] which are also less than ours.

Kinetics of the DC-Conductivity Degradation. For applications such as tissue engineering and chemical sensors, it is important that the blend mat possesses a good electrical conductivity with long-term stability. However, it is well documented in literature that the conductivity of inherently conductive polymers degrades with time because of the segregation of dopants from the emeraldine salt.[56–58]

So, in order to perform the kinetic study of the degradation of the DC-conductivity of our blend nanofiber mats, their DC-conductivity (σ) was measured during 30 weeks (one measurement per week). Blend nanofiber mats were stored in closed vessels in the dark to prevent any eventual influence of humidity and light. Each mat was periodically tested with the four-probe device to measure its DC-conductivity. Then, it was re-desiccated to eliminate any traces of humidity and stored again. Measurements were taken at room temperature (24 °C).

Figure 6(a) illustrates the typical values of ln(σ) as a function of time (week). The curve to be fitted can be expressed by an equation of the form $\sigma = \sigma_0 \exp[-(t/\tau)]$, where ($\sigma_0 = 0.096$ S/cm) is the initial conductivity and ($\tau = 13.031$ week) is the characteristic aging time of σ. This means that, 13 weeks later,

the mat still conserves about 37% of its original conductivity. The slight decrease in the DC conductivity is expressed by the large value of τ (~2200 h). The degradation of the conductivity of the doped PANI in the blend nanofiber mat is attributed, as we mentioned before, to the segregation of the dopants from the polymer backbones.[56–58] This phenomenon is highly noticeable at high annealing temperatures.[59–62] The segregation of dopants leads to deprotonation of the emeraldine salts in the blend mat and this can occur during the storage of the mats even under more conservative conditions.[63]

Electrical Impedance Spectroscopy (EIS). Figure 6(b) depicts the Nyquist plot of PLLA/PANI blend nanofiber mat with the appropriate equivalent circuit in the range 5 Hz–13 MHz. The plot consists of a semicircle extended from the high frequency region to the low frequency region. The diameter of the semicircle represents the electrode resistance which arises from the charge transfer resistance (R_{ct}) in the PLLA/PANI blend nanofiber mat.[2,64–67] The absence of any ascending line in the low frequency region reflects the weak influence of the double layer capacitance (C_{dl}).[66] We note here that the intercept of the real axis at high frequency gives the ohmic series resistance (R_s) between the mat and the aluminum electrode which is negligible compared with R_{ct} where $R_s = 2.3\ \Omega$ since aluminum is an excellent conductive metal.

Fitting the other elements values of the equivalent circuit gives $R_{ct} = 2806\ \Omega$, and $C_{dl} = 18.92$ nF which is a very small capacitance value. The impedance for R//C circuit is given by the equation $Z(j\omega)=R_{ct}/(1+j\omega R_{ct}\ C_{dl})$ where $\omega=2\pi f$. Thus, the term $(j\omega R_{ct}\ C_{dl})$ in the $Z(j\omega)$ plays a very limited role, this explains the dominant ohmic behavior of the system.[66] The value of the dielectric constant of the blend mat at $f=3$ kHz can be deduced from the value of C_{dl}, where we find $\varepsilon_r=13.68$. Comparing this value with that of PANI emeraldine salt ($\varepsilon_r \approx 115$)[68] and that of PLLA ($\varepsilon_r \approx 3$),[69] at the same frequency value, we see that the ε_r value of the blend nanofiber mat is very appropriate as the weight percent of PANI in the mat is 40% and the porosity of the mat of such fiber diameters can reach 70%.[70,71] Bode plot and the related discussion is provided in the Supporting Information.

CONCLUSION

In this work, we presented a new two-step approach to prepare PLLA/PANI blend nanofiber mats. The content of PANI:*p*-TSA in the spinnable solution is high and tunable. Furthermore, the spinnable solution needs no filtration prior to the electrospinning process.

The first step of the approach is the preparation of nonagglomerated powder of PANI:*p*-TSA using ethanol as a dispersing agent of PANI during the redoping process with *p*-TSA. The second is the optimization of the electrospinning parameters and the composition of the spinnable solution. The adequate quantities of *m*-cresol/DCM mixture used for the spinnable solution of PLLA/PANI allow the preparation of a blend nanofiber mat from these two polymers with 40% wt of PANI.

The enhanced values of the DC-conductivity of the prepared mats can be attributed to the use of *m*-cresol that plays the role of a secondary dopant, and to the high content of PANI in the mat.

It is worthy to note that good tuning of *m*-cresol quantities that increases the solubility of PANI in the spinnable solution with its effect on the conformation of PANI chains, and the good optimization of electrospinning parameters, were the key issues to obtain a blend nanofiber mats with such enhanced electrical conductivities.

The effect of aging on the DC-conductivity follows an exponential decrease with a characteristic time of $\tau \approx 13$ weeks. The electrical impedance spectroscopy (EIS) shows pure ohmic behavior of the blend mat. The prepared blend mats are promising candidates for applications that require tunable conductivity such as biomedical materials, sensors, and actuators.

ACKNOWLEDGMENTS

The authors would like to thank Professor M.D. Kubeitari (HIAST-Syria) who generously offered the possibility to use the capacitive impedance cell in order to carry out the electrical impedance measurements of the prepared mats.

REFERENCES

1. Mayukh, M.; Jung, I. H.; He, F.; Yu, L. *J. Polym. Sci. B: Polym. Phys.* **2012**, *50*, 1057.
2. Peng, S.; Zhu, P.; Wu, Y.; Mhaisalkar, S. G.; Ramakrishna, S. *RSC Adv.* **2012**, *2*, 652.
3. Kumar, P. S.; Sundaramurthy, J.; Sundarrajan, S.; Babu, V. J.; Singh, G.; Allakhverdiev, S. I.; Ramakrishna, S. *Energy Environ. Sci.* **2014**, *7*, 3192.
4. Wang, Q.; Zhu, L. *J. Polym. Sci. B: Polym. Phys.* **2011**, *49*, 1421.
5. Lange, U.; Roznyatovskaya, N. V.; Mirsky, V. M. *Anal. Chim. Acta* **2008**, *614*, 1.
6. Janata, J.; Josowicz, M. *Nat. Mater.* **2003**, *2*, 19.
7. Bay, L.; Jacobsen, T.; Skaarup, S.; West, K. *J. Phys. Chem. B* **2001**, *105*, 8492.
8. Smela, E. *Adv. Mater.* **2003**, *15*, 481.
9. Huh, D. H.; Chae, M.; Bae, W. J.; Jo, W. H.; Lee, T. W. *Polymer* **2007**, *48*, 7236.
10. Dhawan, S.; Singh, N.; Venkatachalam, S. *Synth. Met.* **2002**, *129*, 261.
11. Koul, S.; Chandra, R.; Dhawan, S. *Polymer* **2000**, *41*, 9305.
12. Rahman, N. A.; Feisst, V.; Dickinson, M. E.; Malmström, J.; Dunbar, P. R.; Travas-Sejdic, J. *Mater. Chem. Phys.* **2013**, *138*, 333.
13. Mi, H.; Zhang, X.; Yang, S.; Ye, X.; Luo, J. *Mater. Chem. Phys.* **2008**, *112*, 127.
14. Zhang, Y.; Rutledge, G. C. *Macromolecules* **2012**, *45*, 4238.
15. Wessling, B. *Polymers* **2010**, *2*, 786.
16. Huang, J.; Kaner, R. B. *Angew. Chem.* **2004**, *116*, 5941.
17. Zhang, X.; Chan-Yu-King, R.; Jose, A.; Manohar, S. K. *Synth. Met.* **2004**, *145*, 23.
18. Li, X. Q.; Liu, W. W.; Liu, S. P.; Li, M. J.; Ge, M. Q. *Chin. Chem. Lett.* **2014**, *25*, 83.

19. Al-Jallad, M.; Atassi, Y.; Mounif, E.; Tcharkhtchi, A. *J. Appl. Polym. Sci.* **2015**, *132*, DOI: 10.1002/app.41618.
20. Gizdavic-Nikolaidis, M.; Ray, S.; Bennett, J.; Swift, S.; Bowmaker, G.; Easteal, A. *J. Polym. Sci. A: Polym. Chem.* **2011**, *49*, 4902.
21. Karim, M. R. *Synth. Met.* **2013**, *178*, 34.
22. McKeon, K.; Lewis, A.; Freeman, J. *J. Appl. Polym. Sci.* **2010**, *115*, 1566.
23. Prabhakaran, M. P.; Ghasemi-Mobarakeh, L.; Ramakrishna, S. *J. Biosci. Bioeng.* **2011**, *112*, 501.
24. da Silva, A. B.; Bretas, R. E. *Synth. Met.* **2012**, *162*, 1537.
25. Picciani, P. H.; Soares, B. G.; Medeiros, E. S.; de Souza, F. G.; Wood, D. F.; Orts, W. J.; Mattoso, L. H. *Macromol. Theory Simul.* **2009**, *18*, 528.
26. Zhang, H. Q. *Adv. Mater. Res.* **2011**, *332*, 317.
27. Bhadra, S.; Khastgir, D.; Singha, N. K.; Lee, J. H. *Prog. Polym. Sci.* **2009**, *34*, 783.
28. Palaniappan, S.; Amarnath, C. A. *React. Funct. Polym.* **2006**, *66*, 1741.
29. Abdul Rahman, N.; Gizdavic-Nikolaidis, M.; Ray, S.; Easteal, A. J.; Travas-Sejdic, J. *Synth. Met.* **2010**, *160*, 2015.
30. Picciani, P. H.; Medeiros, E. S.; Pan, Z.; Wood, D. F.; Orts, W. J.; Mattoso, L. H.; Soares, B. G. *Macromol. Mater. Eng.* **2010**, *295*, 618.
31. Serrano, W.; Meléndez, A.; Ramos, I.; Pinto, N. *J. Polym.* **2014**, *55*, 5727.
32. Qazi, T. H.; Rai, R.; Dippold, D.; Roether, J. E.; Schubert, D. W.; Rosellini, E.; Barbani, N.; Boccaccini, A. R. *Acta Biomater.* **2014**, *10*, 2434.
33. Xu, P.; Xu, X.; Cui, J.; Li, W.; Wang, G. In 3rd International Conference on Biomedical Engineering Informatics; IEEE, Yantai **2010**, pp 1719–1722.
34. Liu, M.; Zhang, Y.; Zhou, C. *Appl. Clay Sci.* **2013**, *75*, 52.
35. Chen, C. H. *J. Appl. Polym. Sci.* **2003**, *89*, 2142.
36. Lee, K. H.; Park, B. J.; Song, D. H.; Chin, I. J.; Choi, H. *J. Polym.* **2009**, *50*, 4372.
37. Wise, D. L. In Electrical and Optical Polymer Systems: Fundamentals: Methods and Applications; Marcel Dekker, Inc.: New York **1998**.
38. Veluru, J. B.; Satheesh, K.; Trivedi, D.; Ramakrishna, M. V.; Srinivasan, N. T. *J. Eng. Fibers Fabrics* **2007**, *2*, 25.
39. Serrano, W.; Melendez, A.; Ramos, I.; Pinto, N. J. In 9th Ibero-American Congress on Sensors (IBERSENSOR); IEEE: Bogota **2014**, pp 1–4.
40. Gualandi, C.; Govoni, M.; Foroni, L.; Valente, S.; Bianchi, M.; Giordano, E.; Pasquinelli, G.; Biscarini, F.; Focarete, M. L. *Eur. Polym. J.* **2012**, *48*, 2008.
41. Bilbao-Sainz, C.; Chiou, B. S.; Valenzuela-Medina, D.; Du, W. X.; Gregorski, K. S.; Williams, T.; G.; Wood, D. F.; Glenn, G. M.; Orts, W. J. *Eur. Polym. J.* **2014**, *54*, 1.
42. Zhou, H.; Nabiyouni, M.; Lin, B.; Bhaduri, S. B. *Mater. Sci. Eng. C* **2013**, *33*, 2302.
43. Zong, X.; Kim, K.; Fang, D.; Ran, S.; Hsiao, B. S.; Chu, B. *Polymer* **2002**, *43*, 4403.
44. Cui, W.; Li, X.; Zhou, S.; Weng, J. *J. Appl. Polym. Sci.* **2007**, *103*, 3105.
45. Yang, L.; Chen, X.; Jing, X. *Polym. Degrad. Stabil.* **2008**, *93*, 1923.
46. Sonseca, A.; Peponi, L.; Sahuquillo, O.; Giménez, E. *Polym. Degrad. Stab.* **2012**, *97*, 2052.
47. Li, M.; Guo, Y.; Wei, Y.; MacDiarmid, A. G.; Lelkes, P. I. *Biomaterials* **2006**, *27*, 2705.
48. Shameli, K.; Ahmad, M. B.; Yunus, W. M. Z. W.; Ibrahim, N. A.; Rahman, R. A.; Jokar, M.; Darroudi, M. *Int. J. Nanomed.* **2010**, *5*, 573.
49. Bocchini, S.; Frache, A. *Exp. Polym. Lett.* **2013**, *7*, 431.
50. Jeevananda, T.; Lee, J. H. *Mater. Lett.* **2008**, *62*, 3995.
51. Huang, L.; Zhuang, X.; Hu, J.; Lang, L.; Zhang, P.; Wang, Y.; Chen, X.; Wei, Y.; Jing, X. *Biomacromolecules* **2008**, *9*, 850.
52. Ratheesh, R.; Viswanathan, K.; Kumar, L.; Chaudhary, J.; Mishra, A.; Jogdand, A.; Kadam, P.; Aljaff, P.; Rasheed, B. O.; Salh, D. M. *J. Appl. Phys.* **2014**, *6*, 1.
53. Stejskal, J.; Prokeš, J.; Trchová, M. *React. Funct. Polym.* **2008**, *68*, 1355.
54. Low, K.; Horner, C. B.; Li, C.; Ico, G.; Bosze, W.; Myung, N. V. *J. Sens. Actuators B Chem.* **2015**, *207*, 235.
55. Tao, X. Wearable Electronics and Photonics; CRC Press, Boca Raton, **2005**.
56. Lu, X.; Ng, H. Y.; Xu, J.; He, C. *Synth. Met.* **2002**, *128*, 167.
57. Cui, B.; Qiu, H.; Fang, K.; Fang, C. *Synth. Met.* **2007**, *157*, 11.
58. Bernasik, A.; Haberko, J.; Włodarczyk-Miśkiewicz, J.; Raczkowska, J.; Łużny, W.; Budkowski, A.; Kowalski, K.; Rysz, J. *Synth. Met.* **2005**, *155*, 516.
59. Lu, X.; Tan, C. Y.; Xu, J.; He, C. *Synth. Met.* **2003**, *138*, 429.
60. Trchová, M.; Šeděnková, I.; Tobolková, E.; Stejskal, J. *Polym. Degrad. Stabil.* **2004**, *86*, 179.
61. Vitoratos, E. *Curr. Appl. Phys.* **2005**, *5*, 579.
62. Dalas, E.; Sakkopoulos, S.; Vitoratos, E. *Synth. Met.* **2000**, *114*, 365.
63. Huang, W.; MacDiarmid, A. *Polymer* **1993**, *34*, 1833.
64. Xiao, Y.; Lin, J. Y.; Wu, J.; Tai, S. Y.; Yue, G.; Lin, T. W. *J. Power Sour.* **2013**, *233*, 320.
65. Chaudhari, S.; Sharma, Y.; Archana, P. S.; Jose, R.; Ramakrishna, S.; Mhaisalkar, S.; Srinivasan, M. *J. Appl. Polym. Sci.* **2013**, *129*, 1660.
66. Guan, H.; Fan, L. Z.; Zhang, H.; Qu, X. *Electrochim. Acta* **2010**, *56*, 964.
67. Patil, D.; Shaikh, J.; Dalavi, D.; Kalagi, S.; Patil, P. *Mater. Chem. Phys.* **2011**, *128*, 449.
68. Dinesh, S.; Vivek, D.; Kumar, M. P. *Res. J. Chem. Sci.* **2013**, *3*, 16.
69. Nakagawa, T.; Nakiri, T.; Hosoya, R.; Tajitsu, Y. *IEEE Trans. Ind. Appl.* **2004**, *40*, 1020.
70. Li, L.; Hashaikeh, R.; Arafat, H. A. *J. Membr. Sci.* **2013**, *436*, 57.
71. Liu, F.; Guo, R.; Shen, M.; Wang, S.; Shi, X. *Macromol. Mater. Eng.* **2009**, *294*, 666.